

See discussions, stats, and author profiles for this publication at: <https://www.researchgate.net/publication/257392971>

# Investigating Traffic Flow in The Nagel-Schreckenberg Model

Article · April 2013

---

CITATION

1

READS

7,186

1 author:



[Paul James Wright](#)

University of Glasgow

22 PUBLICATIONS 114 CITATIONS

SEE PROFILE

# Investigating Traffic Flow in The Nagel-Schreckenberg Model

Paul Wright

*School of Physics and Astronomy, University of Southampton, Highfield, Southampton, S017 1BJ*

(Dated: April 26, 2013)

I present the investigation involving two extensions of the cellular automaton based Nagel-Schreckenberg model, the Velocity-Dependent-Randomisation (VDR) model, and the two-lane model for symmetric and asymmetric lane changing rule sets. The study of the VDR model outlines a potential method in extending the lifetime of a metastable state and consequently postponing an inevitable traffic jam by orders of magnitude. The two lane model produces a so called ‘critical’ and ‘sub-critical’ flow which combined cause the collapse of flow at a critical density.

## 1. INTRODUCTION

In the modern world the demand for mobility is increasing rapidly, with the capacities of road networks becoming saturated or even exceeded. In densely populated countries such as the UK, it can be financially or socially unfeasible to expand these road networks. It is therefore vital that the existing networks are used more efficiently.

A cellular automaton (CA) is a so called ‘mathematical machine’ which arises from basic mathematical principles. While cellular automata can be used to model a variety of applications, one of the most extensive uses has been modelling single-lane traffic. The most prominent example of this kind of model was first introduced over 20 years ago by Kai Nagel, and Michael Schreckenberg [1]. The Nagel-Schreckenberg (NaSch) model is a simple probabilistic CA based upon rule 184 (for more information see Appendix A) and was the first model of its kind to account for imperfect human behaviour, which is key when modelling traffic networks. With the help of a suitable model, and relevant extensions, one can make realistic predictions about the development of real traffic situations and use these findings to optimise the efficiency of road networks.

In this paper I study the flow for three different conditions. Sections two and three introduce and study the classic single-lane NaSch model while an important extension of this model, called the Velocity-Dependent-Randomisation model which introduces a slow-to-start rule, is then studied in section four. Finally, sections five and six outline the NaSch model for the case of two lanes.

Relevant applications of the extended Nagel-Schrenkenberg Model include the simulations of the inner-city of Duisburg [2], the Dallas/Fort Worth area in the USA [3], and most impressively, the OLSIM project [4]. The OLSIM project predicts the traffic within the German state of Nordrhein-Westfalen at present, 30 minutes, and an hour ahead of time.

## 2. A SINGLE LANE MODEL

The classic NaSch model consists of a one-dimensional grid of  $L$  sites and, in this case, periodic boundary conditions. The sites can be either empty or occupied with

a single vehicle of velocity *zero* to  $v_{max}$  in integer steps. For completeness I recall the rules of the NaSch model for single lane traffic. The NaSch model consists of a set of four rules that must be applied in order, for vehicles from left to right (the direction of travel) and for each iteration (time step) as follows

1. Acceleration: If a vehicle ( $n$ ) has a velocity ( $v_n$ ) which is less than the maximum velocity ( $v_{max}$ ) the vehicle will increase its velocity: if  $v_n < v_{max}; v_n = v_n + 1$ .
2. Braking: If a vehicle is at site  $i$ , and the next vehicle is at site  $i + d$ , and after step 1 its velocity ( $v_n$ ) is greater than  $d$ , the velocity of the vehicle is reduced: if  $v_n \geq d; v_n = d - 1$ .
3. Randomisation (reaction): For a given deceleration probability ( $p$ ) the velocity ( $v_n$ ) of the vehicle ( $n$ ) is reduced:  $v_n = v_n - 1$  for a probability  $p$ .
4. Driving: After steps one through three have been completed for all vehicles, a vehicle ( $n$ ) at a site ( $x_n$ ) advances by a number of steps equal to its velocity: for  $v_n; x_n = x_n + v_n$ .

Steps one through four are based on very general properties of single lane traffic. Step one is based on the intuition of a vehicle to want to travel at the maximum possible velocity,  $v_{max}$ , where acceleration is equal to 1. Step two is a deceleration step in which it assures vehicles do not crash. Step three is vital step in simulating traffic flow as it allows the formation of jams, and is a reaction step. This implies that a vehicle may randomly decelerate for a given deceleration probability,  $p$ . In reality this translates to the driver of a vehicle being distracted, over reacting while braking, or being cautious and leaving a large separation between their vehicle and the vehicle ahead. Given the right conditions this can lead to jam formation. Step four allows vehicles to then advance along the road, this is effectively a time step. An illustration of the steps can be seen in Appendix B.

## 3. A STUDY OF THE SINGLE LANE MODEL

These Monte Carlo simulations have been modelled using Python, for a length of road  $L = 200$  which cor-

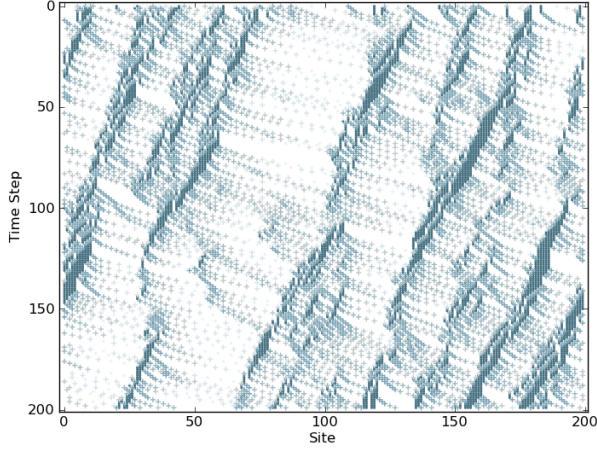


FIG. 1: A space-time diagram for the NaSch Model with  $L = 200$ ,  $p = 0.5$ ,  $\rho = 0.5$ , and 200 time steps. Vehicles are moving to the right, and traffic jams to the left. Darker points indicate a lower the velocity of the vehicle on the road. A white ‘data point’ indicates the lack of a vehicle.

responds to an actual length of 1500m (each site being 7.5m in length). 200 time steps, where each time step is approximately 1 second (an approximation of the reaction time of a driver), and  $v_{max} = 5$  where this corresponds to an actual velocity of  $120 kmh^{-1}$  were also used. The vehicles were distributed randomly along with road with randomly assigned velocities from *zero* to  $v_{max} = 5$ . Figure 1 shows the space-time diagram for the aforementioned conditions with 50 vehicles occupying the road. It can be seen that vehicles are moving to the right with each time step and the darker the point on the space-time diagram, the lower the velocity. The darkest parts of this graph are jams (with velocity  $v = 0$ ), and move in the opposite direction to the vehicles direction of travel. This phenomenon is produced as a vehicle is not affected by the traffic behind it (due to rule 2 in the NaSch model), and hence, causality travels in the opposite direction.

To produce an average velocity vs. global density diagram, and the fundamental (density-flow) diagrams, the global flow and global density need to be calculated. The global density,  $\rho$ , and global flow,  $J(\rho)$ , are defined by equations 1 and 2 respectively.

$$\rho = \frac{N}{L} = \frac{\text{Number of vehicles}}{\text{Number of sites}} \quad (1)$$

$$J(\rho) = \frac{\text{Number of vehicles passing a point}}{\text{Number of time steps}} \quad (2)$$

Due to the random initial distribution of vehicles, global flow is calculated after the initial step due to the initial random configuration needing to settle. The fundamental diagrams were plotted for  $L = 200$ , with 200

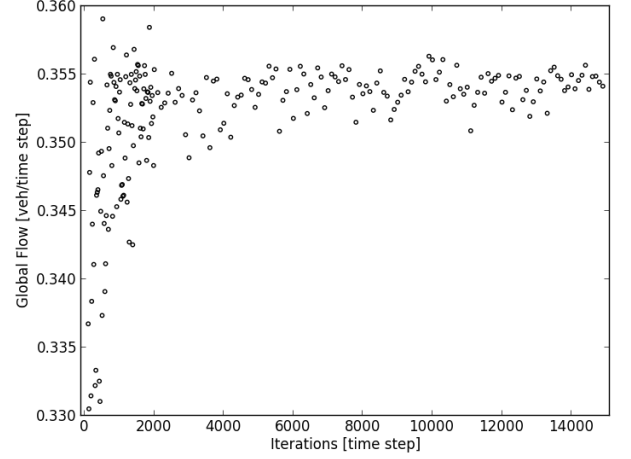


FIG. 2: The number of iterations vs. global flow with  $L = 200$ ,  $p = 0.5$ , and  $v_{max} = 5$ . When flow is calculated for a low number of iterations, large errors are observed without the need for statistical analysis.

iterations,  $v_{max} = 5$  and varying density  $\rho$ , in steps of  $\delta\rho = 0.01$ . However, due to the fluctuations in the calculated flow it was necessary to create a global flow vs. iterations graph to find an ideal number of iterations for  $L = 200$  as seen in figure 2. Observations by eye were sufficient and determined 10000 iterations to be an appropriate value to use with respect to accuracy and computational time (for more information refer to Appendix C).

The first study using the NaSch model was to plot average velocity,  $\langle v \rangle$ , vs. global density,  $\rho$ , for two different values of  $p$ . It can be seen in figure 3 that for both values of  $p$  there is a critical density at which the average velocity is no longer equal to  $v_{max}$ . The flow drops off quickly at the critical density as one would expect. It is also able to show that for a larger value of  $p$  the average velocity of the system collapses at a lower density, and in reality increases the chance of collisions. This increase in  $p$  via a constant distraction explains the need for the Department of Transport to introduce preventative measures against rubbernecking [5]. The results agree with the observations of an actual road [1], and the same pattern is shown for different values of  $v_{max}$  [6]. This allows one to initially determine the maximum density of a road for best flow.

Figures 4 and 5 show the fundamental (density-flow) diagrams for changing  $p$  and  $v_{max}$  respectively. With increasing  $v_{max}$  the dynamics change considerably; note that the relationship for  $v_{max} = 1$  is symmetric due to particle-hole symmetry [7], and this is broken at  $v_{max} > 1$ . The maximum flow tends from rounded to a sharp point with the increase of  $v_{max}$  due to the smaller range of velocities. For figure 4, increasing  $p$  leads to higher fluctuations in velocities and separation between successive vehicles, which in turn results in the collapse

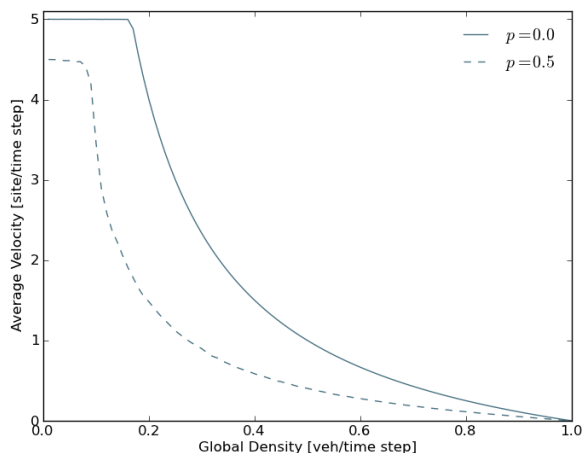


FIG. 3: Average Velocity,  $\langle v \rangle$ , vs. Global Density,  $\rho$ , with  $L = 200$ , 200 iterations,  $v_{max} = 5$  and varying density  $\rho$ , with  $\delta\rho = 0.01$

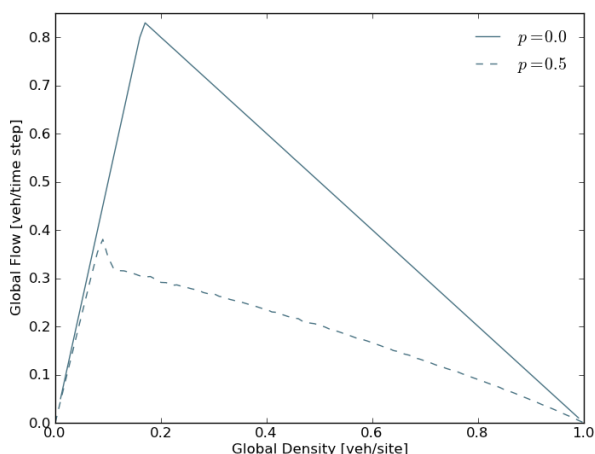


FIG. 4: A fundamental density-flow diagram for the NaSch model with  $L = 200$  sites,  $v_{max} = 5$ , and  $\delta\rho = 0.01$  and varying  $p$ . Measurements were mean measurements over 10000 time steps.

in the flow at lower densities as predicted by figure 3. For an arbitrary value of  $p$ , and very low values of  $\rho$ ,  $\rho \rightarrow 0$ , the flow of traffic is very low,  $J(\rho) \rightarrow 0$ . This can be explained by the low number of vehicles occupying the road, such that nearly no flow exists. As  $\rho \rightarrow 1$ ,  $J(\rho) \rightarrow 0$  because vehicles can hardly move forward. This allows the flow of a given road to successfully predicted from only the global density, the maximum velocity, and the deceleration probability. The physical implications of these regions will be studied in more detail in the following section.

It should also be noted that while figures 4 and 5 agree with T. Held, et al [8], and also general trends obtained

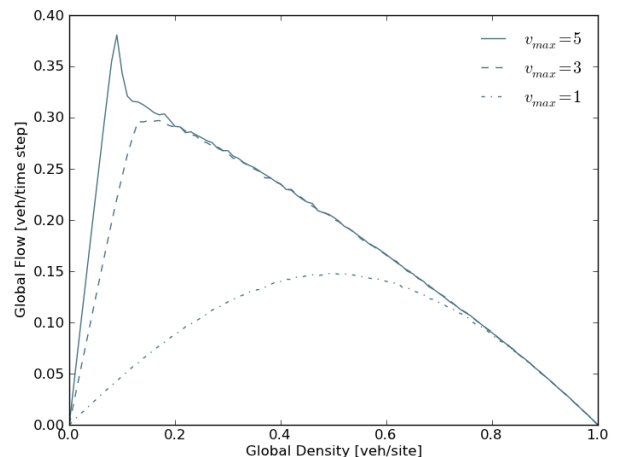


FIG. 5: A fundamental density-flow diagram for the NaSch model with  $L = 200$  sites,  $p = 0.5$ , and  $\delta\rho = 0.01$  and varying  $v_{max}$ . Measurements were mean measurements over 10000 time steps.

by J. Whale, et al [2] there is a slight variation in global flow for  $v_{max} = 5$ ,  $\rho = 0.5$ , at the point of maximum flow. This can be explained as the graphs here were produced using  $L = 200$ , and as a result are affected by the finite size of the road. A system of  $L = 10000$  would be sufficient to exclude these effects [9] but as a consequence uses significantly more computational time (see Appendix B).

More detailed measurements involving road traffic [10][11][12][13] yield the result that flow is not a unique function of density, as these fundamental diagrams suggest. A simple extension of the NaSch model in the next section will update the model to account for such findings. Regardless, the NaSch model is sufficient to model traffic [1] and allows predictions to be made about the maximum flow of a given road, and consequences of vehicle behaviour [2].

#### 4. THE VELOCITY-DEPENDENT-RANDOMISATION (VDR) MODEL

Two types of jams are possible. There are jams that are induced by an external circumstance, such as a bottleneck or lane reductions, and also the spontaneous jams which are caused by fluctuations in vehicle velocities. Spontaneous jams were first shown by T. Treiterer [14] who examined a series of aerial photographs of a highway and it was also shown by B. S. Kerner, et al [15] that phase separated jams and homogeneous metastable states exist. The original NaSch model studied until now doesn't exhibit metastable states or hysteresis. Nor does it exhibit spontaneous, wide phase-separated jams. With a small extension to the original model it is possible to

reproduce these phenomena. This is the VDR model (Barlovic et al [16]) and is based on the NaSch model but with the addition of a slow-to-start rule.

In the VDR model the deceleration parameter,  $p_n(v_n)$ , depends on the velocity,  $v_n$ , of a vehicle,  $n$ . This parameter is calculated in an initial step (now called step 0) and subsequently used in step 3 of the NaSch model. The rule is as follows

0. Determination of the randomisation parameter  $p_n$ , for vehicle  $n$ :

$$p_n(v_n) = \begin{cases} p_0 & \text{for } v_n = 0 \\ p & \text{for } v_n > 0 \end{cases}$$

This is the slow-to-start rule, with two stochastic parameters  $p_0$  and  $p$  which allow the aforementioned phenomena to be reproduced. If a vehicle is stationary ( $v_n = 0$ ) then the vehicle has a probability  $p_0$  that it will not accelerate to  $v_n = 1$  in following time step.

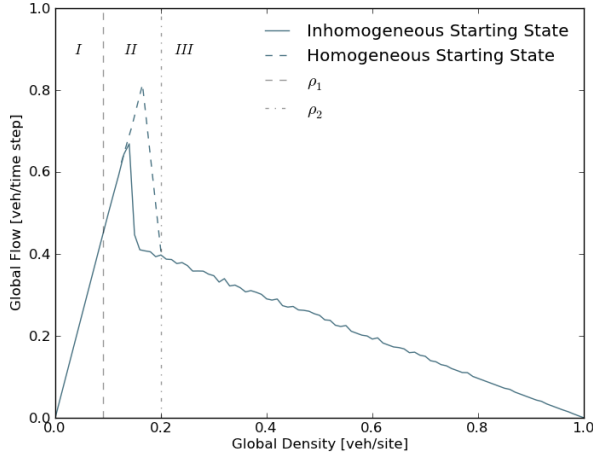


FIG. 6: The fundamental (density-flow) diagram for the VDR model, plotting for homogeneous and inhomogeneous starting conditions with  $L = 200$  sites,  $v_{max} = 5$ ,  $p = \frac{1}{64}$ ,  $p_0 = 0.75$ , and flow averaged over 10000 iterations. The peak of the inhomogeneous branch is due to finite length effects of the road discussed in Appendix C, and is accounted for by the location of  $\rho_1$ .

In this part of the investigation I consider the VDR model with the same parameters as in the NaSch model, but with a deceleration probability  $p = \frac{1}{64}$  for the moving vehicles, and  $p_0 = 0.75$  for the vehicles at rest ( $v_n = 0$ ), and with the addition of the above step. It should be noted that  $p_0 \gg p$ . The inverse of this will produce significantly different results and  $p_0 = p$  reproduces the original NaSch model.

The simulation was implemented for two starting conditions. A homogeneous state, in which all vehicles are equally separated with  $v_{max}$ , and an inhomogeneous state, in which the vehicles are all jammed with  $v_n = 0$  (see figure 7).

The typical fundamental diagram (figure 6) of the VDR model shows three important regions. Region I, in which  $\rho < \rho_1$ , is a free flow regime. For densities up to the  $\rho_1$  no jams with a long lifetime appear [17], and jams that exist in the initial road condition quickly disappear since the outflow from the jam is larger than the inflow (see figure 1). In contrast, in region III, where  $\rho > \rho_2$ , a homogeneous state without jams cannot occur. For region II, the flow  $J(\rho)$  can take on two different states depending on the initial conditions mentioned previously. One is a homogeneous free-flow metastable branch with a long lifetime [8], and the other is a jammed branch with phase separation between the jammed and free-flowing vehicles.

The microscopic structure of the jammed state seen in the VDR model is different to observed jammed states in the NaSch model. The NaSch model contains jammed states with exponential size distribution [18], however, the VDR model shows phase separation.

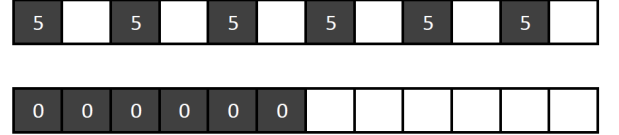


FIG. 7: The homogenous starting state of a road at which all vehicles start equally distant with  $v_{max}$ , and the inhomogeneous starting state of the road where all vehicles are jammed with a velocity  $v = 0$ . This situation is demonstrated for a length  $L = 12$ , and  $\rho = 0.5$

The appearance of a spontaneous, wide phase-separated jam can be seen in figure 8 which is able to show that the density in the outflow region of the jam is reduced compared to the global density. This allows the jam length to grow approximately linearly until the outflow and inflow are in equilibrium (a result of periodic boundary conditions). The jam is formed due to a velocity fluctuation after starting in the homogeneous state. The velocity fluctuation of a single vehicle can cause the vehicle behind to reduce its velocity when the gap between them becomes small ( $d \leq v_n$ ). If the density in the area concerned is large enough this leads to a chain reaction which in turn causes a vehicle to stop, and a jam to form. The time taken for this to happen is the lifetime of the metastable state,  $\tau$ .

The lifetime of the metastable state is shown in figure 9 where **a jam is defined by three stopped vehicles in a row**. It is observed that with the decrease in density the lifetime of the metastable state increases with a more than exponential rate. For a given density, for example  $\rho = 0.2$ , small values of  $v_{max}$  can lead to lifetimes which are greater by orders of magnitude than higher  $v_{max}$ . A system could be implemented in which if a road is found to be in a metastable state the maximum velocity is reduced, therefore reducing the probability of a jam occurring and postponing the inevitable collapse of the



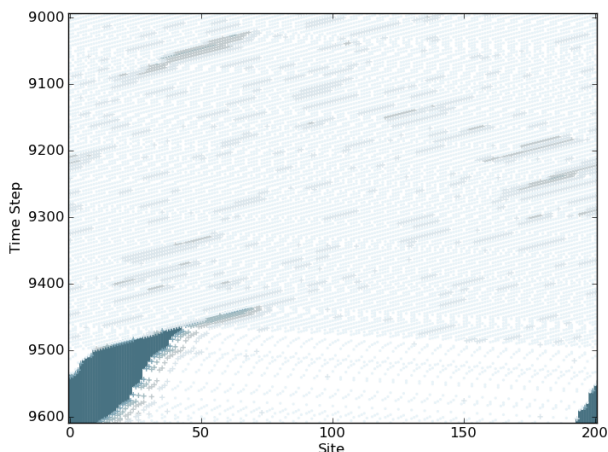


FIG. 8: The spontaneous formation of a jam for  $L = 200$ ,  $v_{max} = 5$ ,  $p = 0.75$ ,  $p_0 = \frac{1}{64}$ , and  $\rho = \frac{1}{6}$ . The darker the point, the lower the velocity, and a white ‘data point’ indicates an empty cell. The homogeneous lifetime is approximately 9450 time steps in this example.

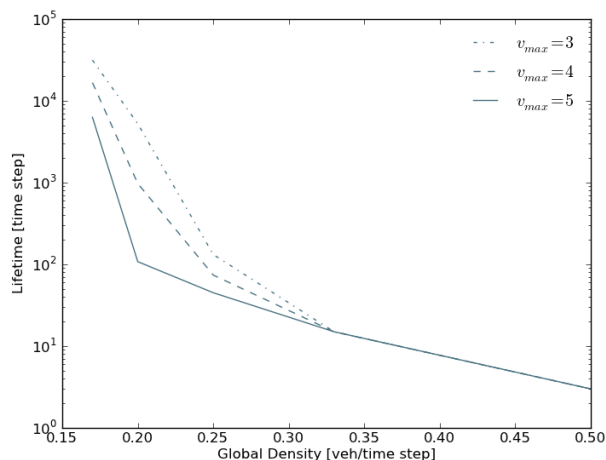


FIG. 9: The lifetime of the metastable state (log scale) vs. Global Density, with  $L = 200$ ,  $p = 0.75$ ,  $p_0 = \frac{1}{64}$ ,  $\delta\rho = 0.01$ , and varying  $v_{max}$ , plotted for means of 100 measurements.

flow into the jammed branch as shown in figure 8.

There are numerous possibilities to extend the VDR model. A distraction in an adjacent lane, the effects of traffic lights or on-off ramps have all been previously studied [8] however, in the next section a two-lane model will be developed.

## 5. THE DEVELOPMENT OF A TWO LANE MODEL

It is necessary to choose an appropriate lane-changing rule set depending on the situation of the experiment. First I consider symmetric lane changing rules which are relevant for US highways and traffic in towns, in which overtaking on both lanes is allowed. The asymmetric rule set describes motorways in the UK, and other European countries. This rule set effectively divides the system into a ‘slow’ and ‘fast’ lane, left and right lanes respectively.

According to the standard set of lane changing rules by other authors, notably [19][20][21][22], the lane changing rules for a symmetric road are as follows.

1. Incentive criterion: If  $v_n \geq d$  it would be more beneficial to transfer lanes (and remain at  $v_n$  rather than braking as in the NaSch model).
2. Safety criterion: For a vehicle to transfer to the adjacent lane, the adjacent site must be unoccupied with  $gap_{lookback} = v_{max}$  and  $gap_{ahead} = v_n$ .

For an asymmetric road, an additional rule, before the ‘Incentive criterion’ is also present.

0. Intuition step: A vehicle prefers to be in the left lane (slow lane).

These rules then replace rule 2 of the NaSch model.

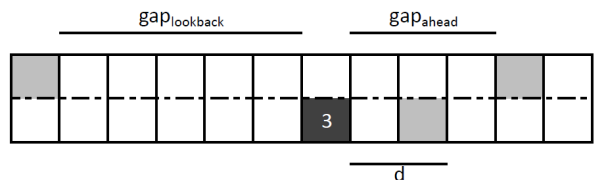


FIG. 10: An example of the two-lane model with vehicles moving to the right. The dark grey hatched cell is the vehicle attempting to change from the right, to left lane (with  $v_n = 3$ ), while the light grey hatched cells are other vehicles on the two-lane road

An example of the conditions being satisfied is given in figure 10. The first of the lane changing rules is due to a vehicle approaching another vehicle from behind. In the NaSch model this vehicle would decelerate ( $v_n = d - 1$ ), but here, it is given the opportunity, as long as the second rule is satisfied, that it can change lanes and carry on at the same velocity,  $v_n$ . The second rule assures a vehicle can initially get into the adjacent lane and makes sure that a vehicle has enough space behind it to pull out and not cause a collision or excessive deceleration with a vehicle travelling at  $v_n = v_{max}$ . It also checks that there is enough space ahead such that it can move forward without the same consequences. After these steps have taken place the normal NaSch rule set is then implemented to move traffic forward in time.

The numerical simulations started with a  $2 \times (L = 200)$  lattice. The velocities of the vehicles were distributed randomly from *zero* to  $v_{max} = 5$  ( at random positions on both lanes) as in the single lane model, and active lane changes now allow the vehicles to attempt to travel at their desired velocity ( $v_{max}$ ) by overtaking.

## 6. A STUDY OF THE TWO LANE MODEL

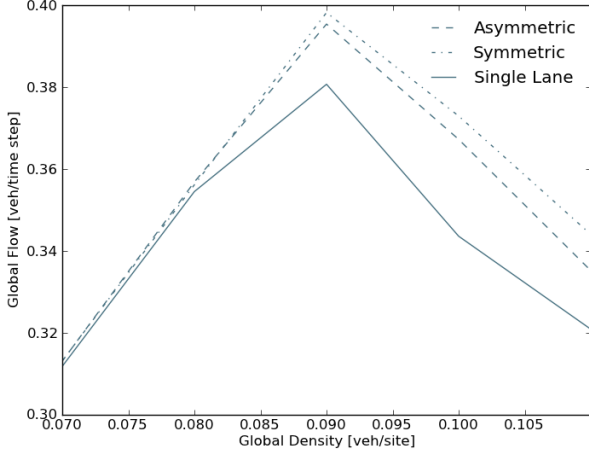


FIG. 11: A fundamental density-flow diagram for the symmetric, and asymmetric two lane models, plotted against the single lane model for comparison, with a  $2 \times L = 200$  lattice,  $v_{max} = 5$ ,  $p = 0.5$ , and  $\delta\rho = 0.01$  for means of 10000 iterations.

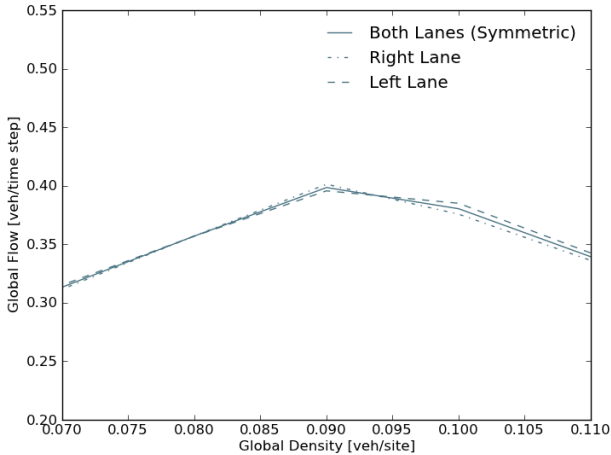


FIG. 12: A fundamental density-flow diagram for the symmetric two lane model with the with a  $2 \times L = 200$  lattice,  $v_{max} = 5$ ,  $p = 0.5$ , and  $\delta\rho = 0.01$  for means of 10000 iterations. The left and right lanes are plotted against the combination of them.

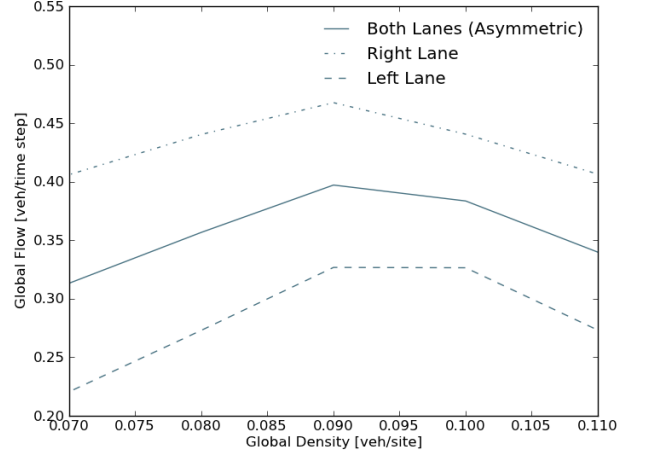


FIG. 13: A fundamental density-flow diagram for the asymmetric two lane model with the with a  $2 \times L = 200$  lattice,  $v_{max} = 5$ ,  $p = 0.5$ , and  $\delta\rho = 0.01$  for means of 10000 iterations. The left and right lanes are plotted against the combination of them.

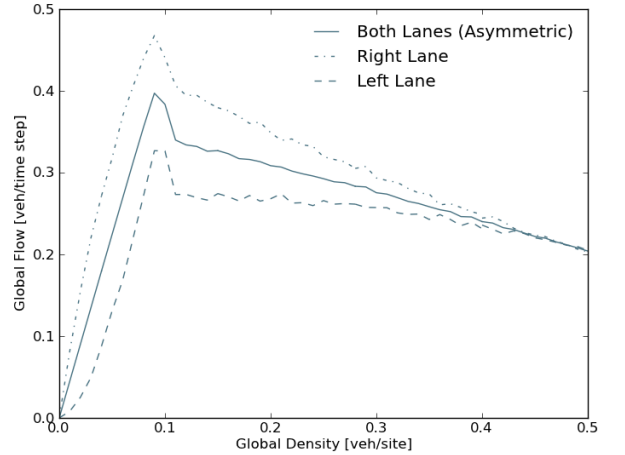


FIG. 14: A fundamental density-flow diagram for the asymmetric two lane model with the with a  $2 \times L = 200$  lattice,  $v_{max} = 5$ ,  $p = 0.5$ , and  $\delta\rho = 0.01$  for means of 10000 iterations. The left and right lanes are plotted against the combination of them.

Figure 11 is the fundamental diagram for the symmetric, and asymmetric models plotted against the single lane model, with the individual lanes for both the symmetric and asymmetric models being plotted in figures 12 and 13. The simulations carried out reproduce well known results, for example, a visible increase of the maximum flow per lane as compared to the single lane NaSch model is observed, and that the symmetric model produces a larger flow than the asymmetric model [23]. From this figure it is also possible to conclude that for both the symmetric and asymmetric models the flow is more than

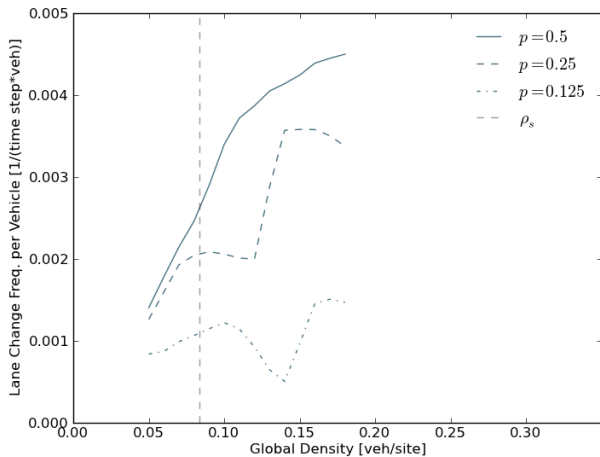


FIG. 15: Lane Change Frequency per Vehicle vs. Global Density for the region near  $\rho_s$ , and displayed in a larger region for emphasis on the local maxima, and minima.

twice that of the single lane model. The asymmetric model shows that the left lane (slow lane) is more highly occupied, and hence has a lower flow than the right lane (fast lane). As seen in figure 13, it also follows that the flow in the left and right-hand lanes of the symmetric model is, on average, higher than the fast lane in the asymmetric model. In the symmetric model the point of maximum flow is  $J(\rho) = 0.40$ , for a density of  $\rho = 0.09$ . Ideally every road would have maximum flow. However, this isn't the case, but density-flow diagrams, when plotted for a variety of lane numbers, can aid in design of new roads as a highway engineer would be able to decide the optimal number of lanes with respect to the predicted number of vehicles likely to be using the road at any one time.

Even though a symmetric two-lane model has higher flow than an asymmetric model, there are valid justifications for deciding on an asymmetric model. For instance, if a three lane US highway is considered, a vehicle in the central lane can have vehicles overtaking in both the left and right lanes, and therefore pulling in from both of these lanes. One can therefore make the hypothesis that under the same conditions, the probability of collisions is higher, and is a downfall in an otherwise efficient lane changing rule set.

It is observed from figure 14 that for the asymmetric model, at low densities, the flow on the left lane builds up slowly with quadratic growth ( $J(\rho) \propto \rho^2$ ). This is what should be expected given two vehicles have to be close enough to force one of them into the left lane. It is also observed, that for  $\rho > 0.4$  the flows observed on both lanes in the asymmetric model are similar, and very similar to the flow found in the symmetric model. Most interestingly, the flow on the left lane keeps increasing slightly past  $\rho_{max} = 0.09$  (figure 13), however, this is cancelled out by the flow for the right lane. These two observations

lead to a hypothesis that the maximum flow observed in the asymmetric case is dependent on a 'critical' flow observed in the right lane, and a 'sub-critical' flow in the left lane. Further investigations should be carried out to clarify the observations reported here, however, due to the combined flow of both the left and right hand lanes in the case of asymmetric and symmetric lane changing rules having the similar values of flow at  $\rho_{max} = 0.09$ , and taking a similar appearance, this implies the overall density is a robust quantity.

A subsidiary investigation of the symmetric two-lane model shows an interesting result. Figure 15 shows the lane changing behaviour in the symmetric two-lane model for varying deceleration probabilities,  $p$ . For lane changing to occur at  $v_{max}$ ,  $2v_{max} + 1$  empty cells need to be present on the adjacent road. It can be easily derived that a local maximum of lane-changing frequency near  $\rho_s$  as defined in equation 3

$$\rho_s = \frac{1}{2} \frac{1}{v_{max} + 1} \quad (3)$$

should be observed. As the braking probability decreases,  $p \rightarrow 0$ , the local maximum becomes more pronounced. It's possible to understand this as for  $p \rightarrow 0$ , where it is observed that for  $\rho = \frac{1}{v_{max} + 1}$  the vehicles are ordered with a gap of length  $v_{max}$  between two vehicles. This implies that the incentive and safety criterion, as defined in the overtaking rules will never be fulfilled. This will result in the lanes being completely decoupled as may be expected under the rule set. It therefore follows that for larger values of  $p$ , there is a more prominent fluctuation between two consecutive vehicles, and hence, lane changing is more prominent in the regions where a local minimum was observed at low  $p$ .

## 7. CONCLUSIONS

In this paper, two extensions to the classic Nagel-Schreckenberg model have been discussed, the VDR model, and the study of two-lane traffic under two separate circumstances (symmetric, and asymmetric lane changing rules).

The classic NaSch model is able to simply predict the critical density of road with respect to the flow, and allows general statements about traffic flow modelled using CA to be made, such as the underlying particle-hole symmetry, and how the deceleration probability and maximum velocity influence the fundamental diagrams. The model allows a basic understanding of traffic, and allows simple conclusions to be made which could aid highway engineers in road planning.

The Velocity-Dependent-Randomisation model introduces the prediction of an important region in the density-flow diagram for a one lane traffic model in addition to the two regions already observed in the NaSch model. For low densities ( $\rho < 0.09$ ) it predicts a free



flow regime, and implies no jams with a long lifetime will appear. However, for high densities ( $\rho > 0.2$ ), a homogeneous state without jams cannot occur. In comparison to the classic NaSch model the flow is generally higher and at times can be twice the value found in the original model. The most interesting result of the VDR model is the hysteresis loop, consisting of a homogeneous free flow branch, and a jammed branch. The loop predicts that the flow of a road can be very large in the homogeneous free flow branch, but for given conditions will eventually collapse (after the lifetime of the metastable state) into a wide phase-separated jam with a long lifetime compared to the jams predicted by the classic NaSch model. It was also shown that the collapse of the metastable state can be postponed if the maximum velocity of the road is reduced before the inevitable collapse into a jammed state.

The two lane model revealed some interesting results. Firstly, the predicted flow for the symmetric model is generally larger than that of the asymmetric model, and for both cases, the flow is more than twice that of the single lane model. It could easily be hypothesised that collisions are more likely in the symmetric model due to

the nature of the rule set but without reliable data from roads with exactly the same conditions, bar the rule set, a definite conclusion cannot be made. On the contrary to the symmetric model (in which each lane is effectively independent of each other), in the asymmetric model the maximum flow is observed to be dependent on a ‘critical-flow’ in the so called fast lane and a ‘sub-critical’ flow in the slow lane. This will require more investigation to clarify the findings, but nevertheless, is an interesting result which could potentially allow the so called ‘fast lane’ to be manipulated at this critical density in order to increase the maximum flow of the road.

The results presented here cover only a small fraction of the many possibilities with the extended NaSch model. I have shown an insight into the behaviour of traffic and this paper has produced some interesting and useful results, which with more study can be understood completely. However, the results obtained can allow highway engineers an insight into predicting traffic, and with the known (or predicted) average road density, it would be possible to choose an appropriate number of lanes, or implement velocity restrictions on existing roads.

- 
- [1] K. Nagel, M. Schreckenberg, J. Phys. I France 2, 2221 (1992)
  - [2] J. Wahle, L. Neubert, J. Esser, M. Schreckenberg, A Cellula Automaton Traffic Flow Model For Online Simulation of Traffic (1999)
  - [3] M. Rickert and K. Nagel, Int. J. Mod. Phys. C 8, 483 (1997)
  - [4] Real-time traffic flow simulation in Nordrhein-Westfalen, <http://www.autobahn.nrw.de/>
  - [5] Department of Transport Press Release, <http://pressreleases.dft.gov.uk/content/detail.aspx?ReleaseID=427364&NewsAreaId=2>
  - [6] A. Ebersbach, J. Schneider, I. Morgenstern, Int. J. Mod. Phys. C 12, 1081 (2001)
  - [7] A. Schadschneider, M. Schreckenberg, J. Phys. A 26, L679 (1993)
  - [8] T. Held, S. Bittihn, Cellula automata for traffic simulation - Nagel-Schreckenberg Model (2011)
  - [9] R. Barlovic, L. Santen, A. Schadschneider, M. Schreckenberg, Metastable States in CA models for Traffic Flow (1997)
  - [10] D. Helbing, Phys. Rev. E 55 (1996) R 25-28
  - [11] B.S Kerner, H. Rehborn, Phys. Rev. E 52 (1996) R 1297-1300
  - [12] B.S Kerner, Phys. Rev. Lett. 81 (1998) 3797-3800
  - [13] B.S Kerner, H. Rehborn, Phys. Rev. Lett. 79 (1997) 4030-4033
  - [14] J. Treiterer, Ohio State Technical Report No. PB 246094, (1975)
  - [15] B. S. Kerner and H. Rehborn, Phys. Rev. E 53, 1297 (1996)
  - [16] R. Barlovic, L. Santen, A. Schadschneider, M. Schreckenberg, Eur. Phys. J. B (1998)
  - [17] R. Barlovic, A. Schadschneider, M. Schreckenberg, Phys. A, 294, 3-4, 525 (2001)
  - [18] K. Nagel and M. Paczuski, Phys. Rev. E 51, 2909 (1995)
  - [19] K. Nagel, D. E. Wolf, P. Wagner, and P. Simon, Phys. Rev. E 58, 1425 (1998)
  - [20] W. Knospe, L. Santen, A. Schadschneider, M. Schreckenberg, Phys. A, 265, 614 (1999)
  - [21] K. Nagel, J. Esser, and M. Rickert, in Annual Reviews of Computational Physics, Vol. VII, 151 (2000)
  - [22] D. Chowdhury, L. Santen, and A. Schadschneider, Phys. Rep. 329, 199 (2000)
  - [23] M. Rickert, K. Nagel, M. Schreckenberg, A. Latour, Phys. A, 231, 4, 534 (1996)
  - [24] Cellula Automata, Models for A Discrete World, [www.interciencia.es/PDF/WikipediaBooks/CellAutomata.pdf](http://www.interciencia.es/PDF/WikipediaBooks/CellAutomata.pdf), 49

### Appendix A: Rule 184

Rule 184 is a one dimensional binary cellular automaton rule. As the Nagel-Schreckenberg model is based upon rule 184 it should be possible to reproduce the space-time diagrams of rule 184 for a variety of densities. Using the simulation created, assuming  $v_{max} = 1$ , and  $p = 0.0$  it is possible to reproduce the published diagrams for  $\rho = 0.25, 0.5$ , and  $0.75$  [24]. The data points in the two shades of blue represent  $v_n = 1, 0$  for darkest to lightest respectively. A white 'data point' represents an empty cell.

As the space-time diagrams (figures 16, 17, 18) results obtained agree with what would be expected from rule 184 it is therefore a good confirmation that the rule set is being correctly implemented.

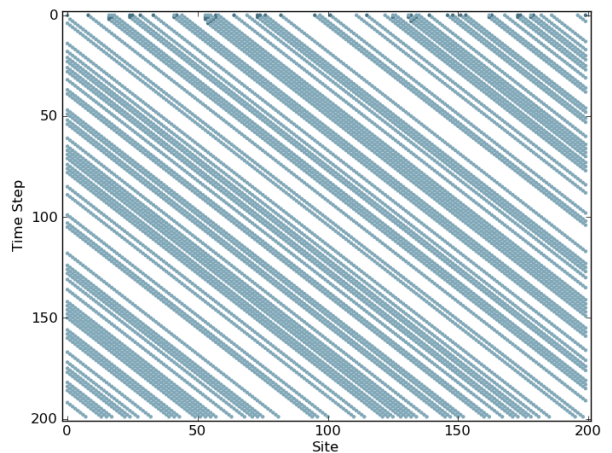


FIG. 16: Rule 184, run for 200 time-steps (iterations) with a random starting arrangement, and a density  $\rho = 0.25$ .

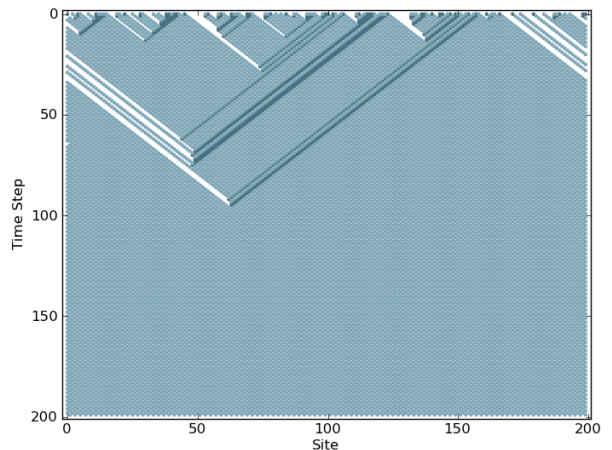


FIG. 17: Rule 184, run for 200 time-steps (iterations) with a random starting arrangement, and a density  $\rho = 0.50$ .

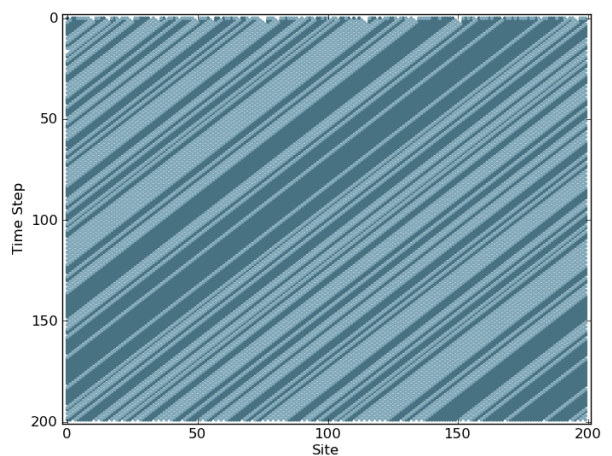


FIG. 18: Rule 184, run for 200 time-steps (iterations) with a random starting arrangement, and a density  $\rho = 0.75$ .

## Appendix B: Implementing The NaSch Rule Set In The Single Lane Model

For completeness and to reduce ambiguity an example of the traffic flow steps, for one iteration (time step) with  $v_{max} = 2$ , and  $L = 8$ . The steps taken by the computer simulation for this example, figure 19, are as follows for steps one through four, and cell sites, 1 through 8 (left to right).

1. Configuration at time  $t$
2. Acceleration ( $v_{max} = 2$ ). The vehicles at sites 3,6, and 7 accelerate by 1.
3. Braking. Vehicles at sites 1, and 6 need to brake.
4. Randomisation ( $p = 0.5$ ). The vehicle at site 1 brakes.
5. Driving. The vehicles drive, and this is the configuration at time  $t+1$ .

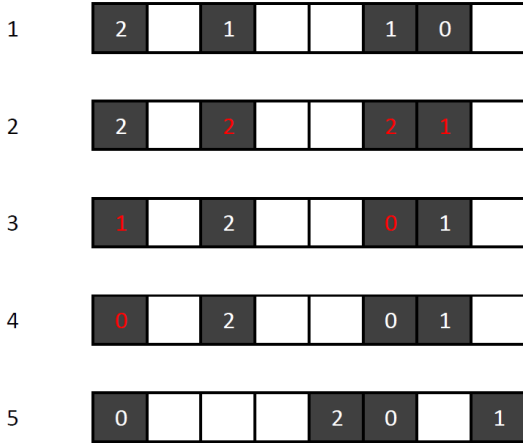


FIG. 19: Implementing the NaSch rule set. The dark grey cells are vehicles and the numbers are the velocities. Changes from one step to the next are highlighted in red.

Where the NaSch rule set is defined as

1. Acceleration: If a vehicle ( $n$ ) has a velocity ( $v_n$ ) which is less than the maximum velocity ( $v_{max}$ ) the vehicle will increase its velocity: if  $v_n < v_{max}$ ;  $v_n = v_n + 1$ .
2. Braking: If a vehicle is at site  $i$ , and the next vehicle is at site  $i + d$ , and after step 1 its velocity ( $v_n$ ) is greater than  $d$ , the velocity of the vehicle is reduced: if  $v_n \geq d$ ;  $v_n = d - 1$ .
3. Randomisation (reaction): For a given deceleration probability ( $p$ ) the velocity ( $v_n$ ) of the vehicle ( $n$ ) is reduced:  $v_n = v_n - 1$  for a probability  $p$ .

4. Driving: After steps one through three have been completed for all vehicles, a vehicle ( $n$ ) at a site ( $x_n$ ) advances by a number of steps equal to its velocity: for  $v_n$ ;  $x_n = x_n + v_n$ .

### Appendix C: A Brief Computational Study For The Single Lane Model

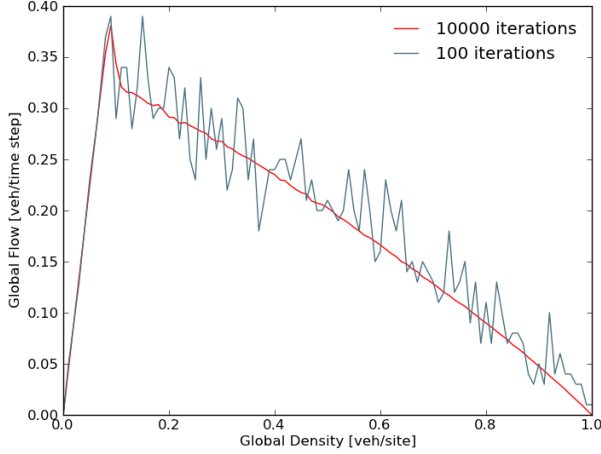


FIG. 20: A fundamental density-flow diagram for the single lane model, with  $L = 200$ ,  $p = 0.5$ , and both 100, and 10000 iterations.

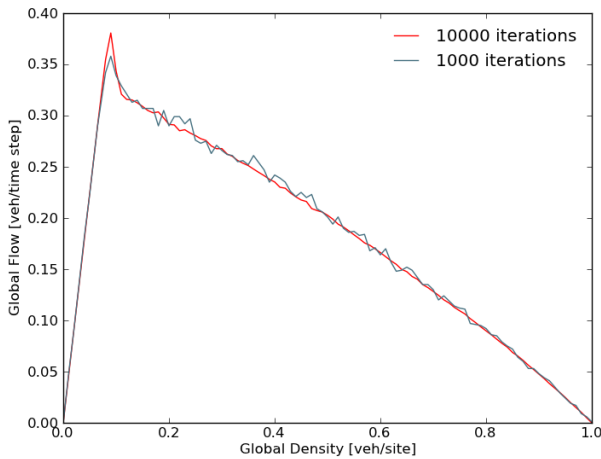


FIG. 21: A fundamental density-flow diagram for the single lane model, with  $L = 200$ ,  $p = 0.5$ , and both 1000, and 10000 iterations.

As briefly discussed in the ‘A Single Lane Model’ section. There are effects on the flow-density diagram due to the finite length of the road, and number of iterations used. In this appendix I include my findings, and justification for using  $L = 200$ , with 10000 iterations.

As shown by figure 2 for a low number of iterations the flow has huge errors (without the need for statistical analysis). Figures 20 and 21 show the density-flow diagrams for 100, 1000, and 10000 iterations, with the initially given  $L = 200$ . It is clear that figure 20 only shows a general trend for 100 iterations, and by using 1000 iterations the uncertainty in the flow is improved

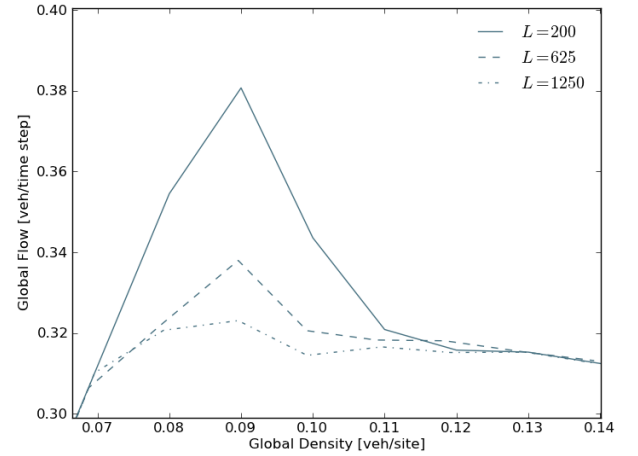


FIG. 22: A fundamental density-flow diagram for the single lane model, with  $p = 0.5$ , 10000 iterations, and  $L = 200, 625, 1250$ .

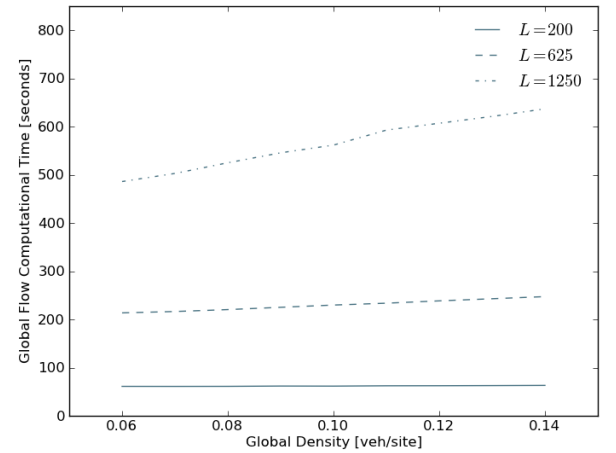


FIG. 23: The computational time needed to calculate the flow at a density  $\rho$ , for values between  $\rho = 0.06$  and  $\rho = 0.14$ , with  $\delta\rho = 0.01$ .

(figure 21). The flow appears stable at 10000 iterations. This project is looking at general trends in traffic simulation data, and 10000 iterations for a length  $L = 200$  is sufficient to reproduce, and improve on, results seen in other papers [8].

In figure 22 I have plotted the flow-density diagram at the point of maximum flow for three different lengths.  $L = 200, 625, 1250$ , where the flow is the mean of 10000 iterations. It is possible to deduce that the ‘peak’ in the original graph, figure 4 is due to a finite length effect, as the peak disappears with increased Length. It would have been ideal to use  $L = 1250$  or greater for the whole paper, but as figure 23 shows there is massive disadvantage by increasing  $L$ , without regard for having

to increase the simulation length as would be required if a change was made.

Figure 23 shows that for plotting the flow for  $\rho = 0.06$ ,  $L = 200$ , takes a mere 60 seconds. However, once you increase that to  $L = 1250$ , the computational times takes a little under 500 seconds to calculate the flow for the given density. By making the crude assumption that it takes 500 seconds to plot each point from  $\rho = 0 \rightarrow \rho = 1.0$  in steps of  $\delta\rho = 0.01$ . The simulation would take 13

hours to produce one graph compared to the one hour it takes for  $L = 200$ .

Using  $L = 200$  is a compromise I took, however, it has no negative effect on the produced graphs as flow is the maximum at the same point, is just a feature that needs to be understood. It should be noted that this effect is seen on other papers [8] who used  $L = 100$ , and 10000 iterations. A paper without this effect used  $L = 10000$ , with  $10^6$  iterations [9].